CHEMICAL ENGINEERING TRANSACTIONS
VOL. 65, 2018
A publication of AIDIC
The Italian Association of Chemical Engineering
Online at www.aidic.it/cet
Guest Editors: Eliseo Ranzi, Mario Costa

ISBN 978-88-95608-62-4; **ISSN** 2283-9216
DOI: 10.3303/CET1865055

Numerical Simulation of Mass Transfer of Slug Flow in Microchannel

Ying Li*, Huanran Lv

Institute of Environmental and Chemical Engineering, Dalian Jiaotong University, Dalian 116028, China
liying630@sina.com

Computational fluid dynamics (CFD) is used to investigate mass transfer characteristics of gas-liquid two-phase slug flow in microchannel. Simulation results illustrates liquid volumetric mass transfer coefficient k_La is proportional to the square root of diffusion coefficient D and gas bubble velocity u_B, and inversely proportional to the length of slug unit cell. Moreover, k_La shows a similar tendency to Higbie penetration model, but has a large deviation. In this paper, an improved expressions including two contributions of the caps and liquid film is presented based on Higbie penetration model. The effect of *Fo* on mass transfer of liquid film contribution is discussed. The predicted k_La with the new correlation agree well with the simulated k_La, the average relative error is within 20%. The control variables which determine slug flow mass transfer in microchannel such as gas bubble velocity u_B、 liquid film thicknessδ_F、 liquid film length L_F and unit cell length L_{UC} can be deduced from superficial gas velocity u_G、 superficial liquid velocity u_L and liquid physical properties. Thus, the developed correlation not only reflects the characteristics of mass transfer process, but also has simplicity and practicality as empirical correlations.

1. Introduction

Microreactor has wide application in gas liquid absorption (Ye et al., 2013) and reaction (Zhao et al., 2013) due to its high efficient mass transfer characteristic. Slug flow in microchannle is an ideal flow pattern to intensify gas liquid mass transfer (Haase et al., 2016; Khramtsov et al., 2016). Slug flow is characterized by the presence of elongated gas bubbles with lengths greater than the capillary diameter, which rise along the capillary separated from each other by liquid slugs. The gas bubbles occupy most of capillary cross section, separated from the channel wall by a thin liquid film. This flow arrangement has been reported to yield superior mass-transfer performance. Liquid side mass transfer coefficient correlation k_La of slug flow in capillaries was presented in eq.(1). It illustrated that k_La relies on the length and speed of liquid slug (Berčrč and Pintar, 1997). k_La of slug flow contains two parts of gas cap and liquid film shown in Eq.(2) and can be calculated through Higbie penetration theory such as Eq.(3) (Van baten and Krishna, 2004). A new colourimetric technique and calculation method were developed to determine the liquid side mass transfer coefficients around the slug bubbles (Dietrich et al., 2013). When residence time was defined as the length of gas bubble divided by gas liquid relative velocity, liquid side mass transfer coefficient was to penetration theory (Haghnegahdar et al., 2016). The contribution of liquid film to mass transfer coefficient was reduced when the residence time was long enough (Abolhasani et al., 2015). A new correlation Eq(4) was developed combined penetration theory and empirical representations (Yue et al., 2009).

$$k_La = 0.111\frac{(u_G+u_L)^{1.19}}{((1-\varepsilon_G)L_{UC})^{0.57}} \tag{1}$$

$$k_La = k_{LC}a_C + k_{LF}a_F \tag{2}$$

$$k_La = \frac{2\sqrt{2}}{\pi}\sqrt{\frac{Du_B}{d_H}}\cdot\frac{4}{L_{UC}} + \frac{2}{\sqrt{\pi}}\sqrt{\frac{Du_B}{\varepsilon_G L_{UC}}}\cdot\frac{4\varepsilon_G}{d_H} \tag{3}$$

Please cite this article as: Li Y., Lv H., 2018, Numerical simulation of mass transfer of slug flow in microchannel, Chemical Engineering Transactions, 65, 325-330 DOI: 10.3303/CET1865055

$$k_L a = \frac{2}{d_H}\left(\frac{Du_B}{L_B + L_S}\right)^{0.5}\left(\frac{L_B}{L_B + L_S}\right)^{0.3} \tag{4}$$

Eq.(3) reflected the mass transfer characteristic of slug flow in microchannel. But the calculation of kLa needed information such as bubble length and velocity and was not convenient for practical application. Many researchers put forward empirical correlations like Eq.(5) (Sobieszuk et al., 2011) and (6) (Yue et al., 2007).

$$Sh = 0.1\mathrm{Re}^{1.12}\, Sc^{0.05} \tag{5}$$

$$Sh_L a d_H = 0.084\,\mathrm{Re}_G^{0.213}\,\mathrm{Re}_L^{0.937}\, Sc_L^{0.5} \tag{6}$$

It is difficult to measure liquid side mass transfer coefficient in the narrow microchannel. Numerical simulation is used to investigate the mass transfer performance of gas liquid two phase flow in microchannels. Combined with the influence of the flow parameters of slug flow on the liquid side mass transfer coefficient in the simulated results and the correlation formula based on the two contributions derived from the Higbie permeation model, an improved correlation formula is proposed to predict the liquid side mass transfer coefficient of slug flow in microchannel.

2. Numerical simulation

2.1 Mathematical model

In microchannel, each gas bubble and liquid slug with the same size constitute one unit cells shown in Figure 1(a). One of the unit cells was intercepted in this study and periodic boundary condition was set at the inlet and outlet in Figure 1(b).

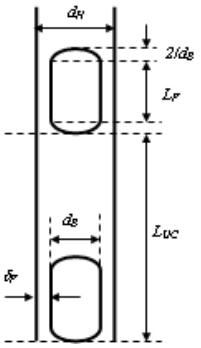

(a)

Figure 1(a) Schematic representation of slug flow in microchannel

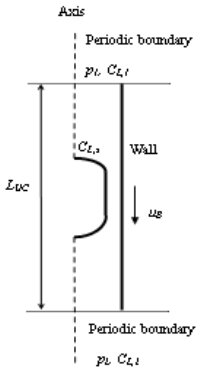

(b)

Figure 1(b) Mathematical model of the unit cell

The volume averaged mass and momentum conservation equations in the Eulerian framework were given by

$$\frac{\partial \rho}{\partial t} + \nabla \cdot (\rho v) = 0 \tag{7}$$

$$\rho \frac{\partial v}{\partial t} + \rho \nabla \cdot (vv) = -\nabla p + \nabla \cdot \tau + \rho g + \vec{F} \tag{8}$$

The boundary condition was periodic in the vertical direction ($u_1 = u_2$; $p_1 = p_2$). Simulations were performed in a reference system in which the bubble was stationary and the wall moved up with the bubble rise velocity u_B. At the outside wall, the boundary condition was set to $u_z = -u_B$, $u_r = 0$, where r and z were the radial and axial coordinates. At the axis of symmetry, we had $du_z/dr = 0$.

The simulations were carried out using axi-symmetric 2D grids using cylindrical coordinates. Mass transfer equation was,

$$\frac{\partial C_L}{\partial t} + \nabla \cdot (v_L C_L - D \nabla C_L) = 0 \tag{9}$$

Here, C_L was the concentration of solute in the liquid phase and D was the diffusion coefficient. At the top and bottom, the periodic boundary conditions were used, $C_{L,1} = C_{L,2}$. Through the outside wall, $dC_L/dr = 0$. Symmetry conditions applied to the center axis, $dC_L = dr = 0$. At the bubble surface, the concentration was specified as $C_{L,s} = 1$.

First, the computational domain of Figure 1(b) was divided into grids. For this irregular area, unstructured mesh was adopted and fined on the surface of bubbles. PISO algorithm was used to solve velocity pressure coupling to ensure computation accuracy while accelerating convergence. In order to prevent numerical diffusion, the QUICK format was used to discrete time convection terms. The whole simulation process was carried out in two steps. First, the steady state simulation was used to solve the mass and momentum conservation equation, and the convergence velocity field was used for the next step of mass transfer simulation. Mass transfer was performed by unsteady state. The time step was 0.0001, and the iteration was 15000 steps. The liquid side mass transfer coefficient $k_L a$ was calculated from:

$$k_L a = \frac{\left(\overline{C}_{L,t_2} - \overline{C}_{L,t_1}\right)/\left(t_2 - t_1\right)}{\left(C_{L,s} - \dfrac{\overline{C}_{L,t_2} + \overline{C}_{L,t_1}}{2}\right)} \qquad \overline{C}_{L,t} = \frac{\sum_{domain} vol_i C_{L,t}}{\sum_{domain} vol_i} \tag{10}$$

$$\left\langle k_L a \right\rangle_\tau = \frac{1}{t}\int_0^t k_L a dt \tag{11}$$

2.2 Numerical simulation

The values of $k_L a$ calculated at each time step using Eq. (11) were shown in Figure 2. After about 1 s $k_L a$ reached a quasi-steady state value. And the simulated $k_L a$ values were independent of the number of grids in Figure 3.

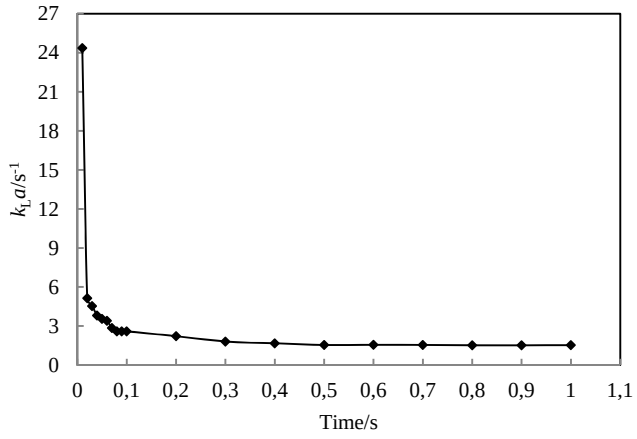

Figure 2 Effect of calculation time on liquid volumetric mass transfer coefficient

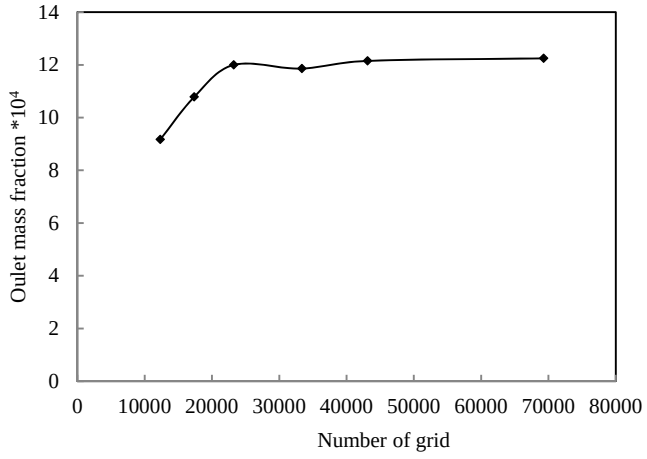

Figure 3 Effect of number of grid on outlet mass fraction of solution absorption

3. Results and discussion

According to the analysis of the experimental data, the basic flow parameters of slug flow in the microchannel were as follows: bubble velocity u_B=0.6m/s, liquid film thickness δ_F=13μm, liquid film length L_F=2mm and slug unit length L_{UC}=6mm. When the size of the slug bubble is larger than the channel characteristic size d_H=300μm, the internal circulation is produced inside the bubble under the shear action between the bubble and the continuous liquid film or the channel wall, which reduces the thickness of the bubble boundary layer and the diffusion distance, increases the contact time and the interface area of gas and liquid, and eventually leads to the intensifying of mass transfer process.

The simulated results fitted well with the experimental results of Yue et al. (2009) in Figure 4. The k_La values were higher one to two orders than traditional gas liquid contactors. Otherwise, the simulated results had large deviation from the results of Dietrich et al. (2013) which overestimated the contribution of liquid film to mass transfer because of the suppose of complete mix between liquid slug and liquid film.

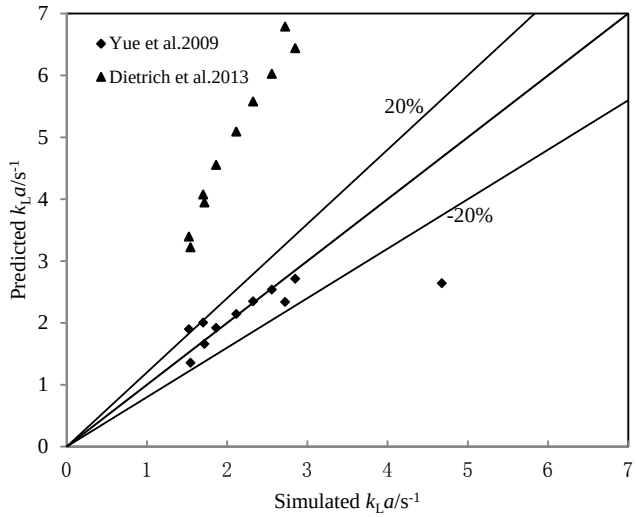

Figure 4 Comparison between the simulated k_La values and predictions of other research

According to simulated results in Figure 5(a),(b) and (c), liquid side mass transfer coefficient was proportional to square root of diffusion coefficient D and square root of bubble velocity u_B, inversely proportional to slug unit length L_{UC}. These tendencies were completely consistent with the predictions of penetration theory. Liquid side mass transfer coefficient increased with the thinning of liquid film in Figure 5(d), which was not expressed in Eq.(3).

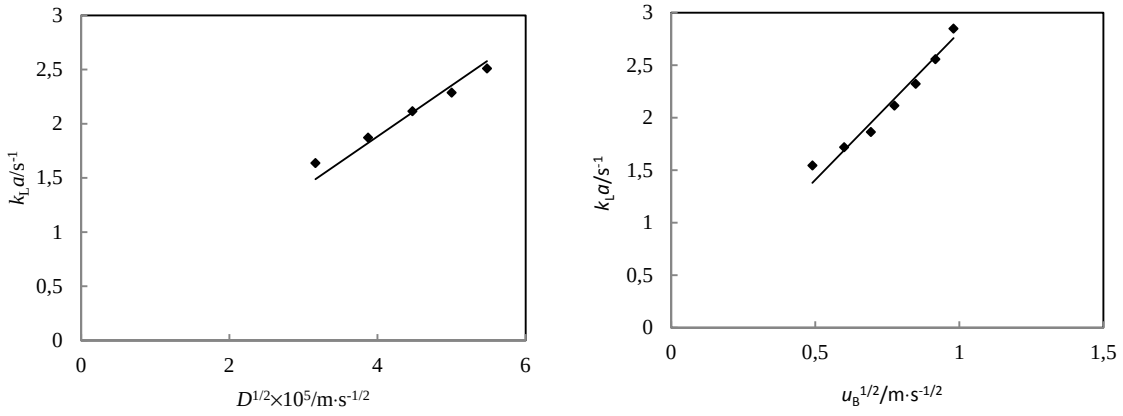

(a) (b)

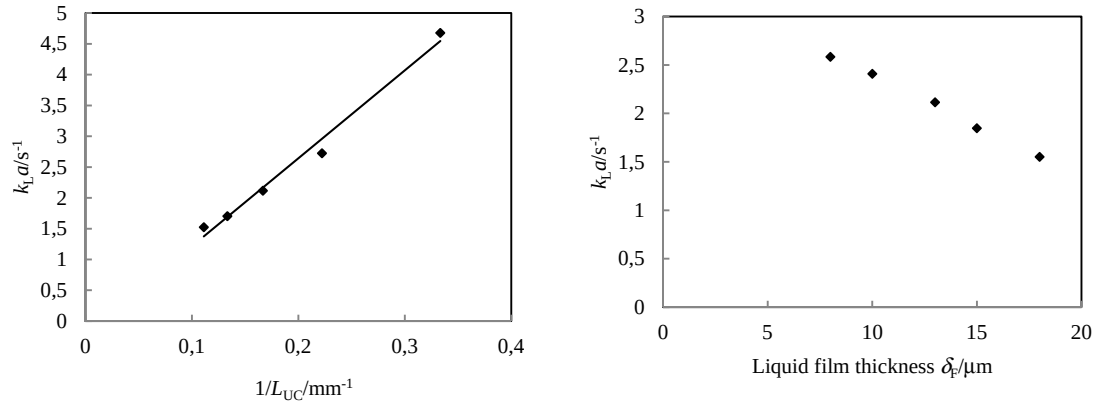

Figure (5) Dependence of the liquid side mass transfer coefficient on (a) diffusion coefficient D, (b) bubble velocity u_B, (c) slug unit length L_{UC} and (d) liquid film thickness δ_F

According to the original penetration theory represented by Eq.(3), the model assumed the presence of a well-mixed liquid phase within the liquid slugs and short contact times at the gas−liquid interface (*Fo* ≪ 1).The contributions of bubble caps and liquid film to liquid side mass transfer coefficient were changeable at different conditions. The correlation in Eq.(3) can be simplified based on the practical application. When *Fo* ($Fo = \frac{DL_B}{u_B \delta_F^2}$) was larger than 1, liquid film was saturated. Thus liquid side mass transfer coefficient was controlled only by liquid slug such as Abolhasani et al.(2015) and the second term in Eq. (3) can be ignored. The contribution of liquid film to mass transfer was effective when *Fo* was between 0.0075-0.074 (Ren et al., 2012). In this study, liquid film was not saturated and *Fo* was between 0.01 and 0.1. The contribution of liquid film to mass transfer can be regressed as function of *Fo*. An improved correlation based on penetration theory was presented in this paper shown in Eq. (12). Liquid side mass transfer coefficient was inversely proportional the exponential function of *Fo* through fitting simulated results. The improved correlation can better predict liquid side mass transfer coefficient with a relative error below 20% in Figure 6.

$$k_L a = \frac{2\sqrt{2}}{\pi}\sqrt{\frac{Du_B}{d_H}}\cdot\frac{4}{L_{UC}} + \frac{2}{\sqrt{\pi}}\sqrt{\frac{Du_B}{L_F}}\cdot\frac{4}{d_H}\cdot\frac{L_F}{L_{UC}}\cdot f(Fo) \qquad f(Fo) = 0.3e^{-Fo} \tag{12}$$

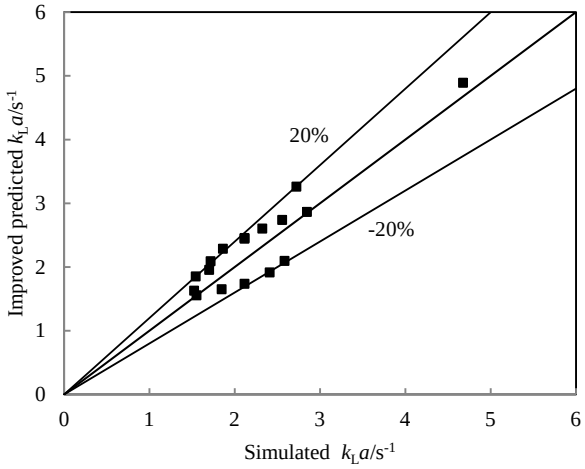

Figure 6 Comparison between the simulated $k_L a$ values and predictions of improve correlation Eq.(12)

4. Conclusions

In this paper, the numerical simulation method was used to calculate the liquid side mass transfer coefficient of the gas liquid two phase flow in microchannel. Simulation results were in good agreement with the experimental results of Yue et al.(2009). According to the simulation results, the relationship between the mass transfer coefficient k_La and the diffusion coefficient D, the bubble velocity u_B and the length of sluf unit length L_{UC} was consistent with the prediction trend of Higbie penetration theory model. Combined with the effect of liquid film thickness on the liquid side mass transfer coefficient, an improved correlation of the two parts of k_La based on the penetration model was proposed. The relative error between prediction results of the new correlation and the simulation results was within 20%.

Acknowledgments

The authors gratefully acknowledge the financial support provided for this work by the New Century Excellent Talents in University of Liaoning Province (Grant no. LJQ2015019) and Natural Science Foundation of Liaoning Province (Grant no. 2015020220).

References

Abolhasani M., Kumacheva E., Günther A., 2015, Peclet Number Dependence of Mass Transfer in Microscale Segmented Gas−Liquid Flow, Industrial & Engineering Chemistry Research, 54, 9046-9051

Berčič G., Pintar A., 1997, The Role of Gas Bubbles and Liquid Slug Lengths on Mass Transport in the Taylor Flow through Capillaries, Chemical Engineering Science, 52(21-22), 3709-3719

Dietrich N., Loubière K., Jimenez M., Hébrard G., Gourdon C., 2013, A New Direct Technique for Visualizing and Measuring Gas-Liquid Mass Transfer around Bubbles Moving in a Straight Millimetric Square Channel , Chemical Engineering Science, 100, 172-182

Haase S., Murzin D. Y., Salmi T., 2016, Review on Hydrodynamics and Mass Transfer in Minichannel Wall Reactors with Gas–Liquid Taylor Flow, Chemical Engineering Research and Design,113, 304-329

Haghnegahdar M., Boden S., Hampel U., 2016, Mass Transfer Measurement in a Square Milli-channel and Comarison with Results from a Circular Channel, International Journal of Heat and Mass Transfer, 101, 251-260

Khramtsov D. P., Vyazmin A. V., Pokusaev B. G., Karlov S. P., Nekrasov D. A ., 2016, Numerical Simulation of Slug Flow Mass Transfer in the Pipe with Granular Layer, Chemical Engineering Transactions, 52, 1033-1038

Rahim N. A. A., Azudin N. Y., Shukor S. R. A., 2017, Computational Fluid Dynamic Simulation of Mixing in Circular Cross Sectional Microchannel, Chemical Engineering Transactions, 56, 79-84

Ren J., He S., Ye C ., Chen G., Sun C., 2012, The ozone mass transfer characteristics and ozonation of pentachlorophenol in a novel microchannel reactor, Chemical Engineering Journal, 210, 374-384

Sobieszuk P., Pohorecki R., Cygaǹski P., Grzelka J., 2011, Determination of the Interfacial Area and Mass Transfer Coefficients in the Taylor Gas-Liquid flow in a Microchannel, Chemical Engineering Science, 66 (23), 6048–6056

Van Baten J. M., Krishna R., 2004, CFD Simulations of Mass Transfer from Taylor Bubbles Rising in Circular Capillaries, Chemical Engineering Science, 59(12), 2535-2545

Ye C., Dang M., Yao C., Chen G., Yuan Q., 2013, Process Analysis on CO_2 Absorption by Monoethanolamine Solutions in Microchannel Reactors, Chemical Engineering Journal, 225, 120-127

Yue J., Chen G. W., Yuan Q., Luo L. A., Gonthier Y., 2007, Hydrodynamics and mass transfer characteristics in gas-liquid flow through a rectangular microchannel, Chemical Engineering Science, 62(7), 2096-2108

Yue J., Luo L., Gonthier Y., Chen G. W., Yuan Q., 2009, An Experimental Study of Air-Water Taylor Flow and Mass Transfer inside Square Microchannels, Chemical Engineering Science, 64(16), 3697-3708

Zhao Y. C., Yao C. Q., Chen G. W., Yuan Q., 2013, Highly Efficient Synthesis of Cyclic Carbonate with CO_2 Catalyzed by Ionic Liquid in a Microreactor, Green Chemistry, 15, 446-452